Uptake of FITC-Chitosan Nanoparticles by A549 Cells

Min Huang,[1] Zengshuan Ma,[1] Eugene Khor,[2] and Lee-Yong Lim[1,3]

Received March 26, 2002; accepted June 21, 2002

Purpose. The objective of this study was to evaluate the extent and mechanism of uptake of fluorescent chitosan nanoparticles by the A549 cells, a human cell line derived from the respiratory epithelium.
Methods. Covalent conjugation with fluorescein-5-isothiocyanate yielded stably labeled chitosan molecules, which were successfully formulated into nanoparticles by ionotropic gelation. Uptake of fluorescein-5-isothiocyanate-chitosan nanoparticles and chitosan molecules by confluent A549 cells was quantified by fluorometry.
Results. Cellular uptake of chitosan nanoparticles was concentration and temperature dependent, having K_m and V_{max} of 3.84 μM and 58.14 μg/mg protein/h, respectively. Uptake of chitosan nanoparticles was up to 1.8-fold higher than that of chitosan molecules alone and was not inhibited by excess unlabeled chitosan molecules. Hyperosmolarity, chlorpromazine and K^+ depletion inhibited by 65, 34, and 54%, respectively, the uptake of chitosan nanoparticles at 37°C, but filipin had no influence on the uptake. Confocal imaging confirmed the internalization of the chitosan nanoparticles by the A549 cells at 37°C.
Conclusions. Formulation of chitosan into nanoparticles significantly improved its uptake by the A549 cells. Internalization of chitosan nanoparticles by the cells seems to occur predominantly by adsorptive endocytosis initiated by nonspecific interactions between nanoparticles and cell membranes, and was in part mediated by clathrin-mediated process.

KEY WORDS: chitosan; nanoparticles; A549 cells; FITC; uptake.

INTRODUCTION

Chitosan, a polycationic polymer comprised of mainly glucosamine units, is known to enhance paracellular permeability and the absorption of hydrophilic molecules in the Caco-2 cell culture model by structural reorganization of the tight junction ZO-1 and cytoskeletal F-actin proteins (1). The modulation of drug transport was, however, inhibited in mucus-secreting epithelial cells (2) and dependent on the polymer retaining its positive charges, which could pose a problem at physiologic pH (3). To overcome these difficulties, chitosan nanoparticulate systems were developed, partly because the nanoparticles could protect a labile drug load from chemical and enzymatic hydrolyzes (4).

Chitosan nanoparticles are potential delivery systems for vaccines, genes, and anticancer agents (5,6). In these applications, the efficiency of drug delivery is less dependent on enhanced paracellular permeability than on the effectiveness with which the drug cargo is taken up intact into the target cell. Nanoparticle-mediated drug transport in absorptive epithelial cells occurs mainly through the vesicular endocytic pathways, which could be mediated by nanoparticle-cell membrane interaction (7). To our knowledge, the endocytosis of chitosan nanoparticles by absorptive cells has not been quantified.

Fluorescently labeled nanoparticles can provide a rapid, simple, and sensitive means to quantify cell-associated nanoparticles by fluorometry (8). However, quantification is possible only if a calibration curve, prepared in the same way as the samples, is used. It is also important that the fluorescent marker is not appreciably dissociated from the nanoparticles to maintain stoichiometry during subsequent processing, storage, and uptake experiments. Markers are known to readily dissociate if they are physically adsorbed onto the surface of preformed particles (9). We have explored the alternative of loading the fluorescent markers, fluorescein sodium and 5,6-carboxyfluorescein, into the chitosan nanoparticles, but found that more than 40% of the loaded markers leached out from the nanoparticles after 5 h of incubation in pH 7.4 phosphate buffer at 37°C. This time-dependent release process could confound the quantification of nanoparticles in cellular uptake experiments.

Two separate groups of researchers have recently conjugated the fluorescent marker, fluorescein isothiocyanate (FITC), to the chitosan molecule and used this derivative to study chitosan-mucin interactions (10) and the biodegradation and distribution of chitosan in mice (11). We hypothesized that the use of this derivative, in which the fluorescent marker was covalently bound to the polymer, would alleviate the problem of marker dissociation from the chitosan nanoparticles and enable the uptake of chitosan nanoparticles to be quantified. In this study, we evaluated the stoichiometry of the FITC-chitosan conjugate, the feasibility of preparing nanoparticles with the conjugate, and the feasibility of assaying the quantity of nanoparticles by fluorometry.

Quantification and elucidation of the mechanism of uptake of the chitosan nanoparticles was performed with confluent A549 cell monolayers, an *in vitro* model of the pulmonary epithelium having the characteristic features of the alveolar Type II cells. Because the fluorophore was conjugated to the chitosan molecule, it was also possible to measure the cellular uptake of the soluble chitosan molecule. This allows a novel comparative evaluation of cellular response to chitosan presented in two forms, soluble macromolecule and condensed nanoparticle.

MATERIALS AND METHODS

Materials

Chitosan hydrochloride (Protasan® CL113), from Pronova Biopolymer (Drammen, Norway), was determined by dilute solution viscometry (12) to have a molecular weight (daltons) of 180,000 ± 7683 (n = 3) and by the first derivative method of UV spectrophotometry (13) to have a degree of deacetylation (DD) of 90.21 ± 0.88% (n = 3). Tripolyphosphate sodium (TPP), acetic acid, FITC, chlorpromazine, filipin, sucrose, Triton X-100, and methanol were purchased from Sigma Chemical Co. (St. Louis, MO, USA), whereas

[1] Department of Pharmacy, National University of Singapore 18 Science Drive 4, Singapore 117543.
[2] Department of Chemistry, National University of Singapore 18 Science Drive 4, Singapore 117543.
[3] To whom correspondence should be addressed. (e-mail: phalimly@nus.edu.sg)

0724-8741/02/1000-1488/0 © 2002 Plenum Publishing Corporation

Sephadex G-50 (medium) was from Amersham Life Science (Little Chalfont, Buckinghamshire, UK). The transport medium was composed of Hanks Balanced Salt Solution (HBSS), buffered with 10 mM *N*-2-hydroxyethylpiperazine-*N*′-2-ethanosulfonic acid (HEPES) and adjusted to pH 6.2 with 1.0 M HCl, all of which were from Sigma. Ultrapure water (Millipore, Bedford, MA, USA) was used throughout. All other chemicals were of the highest grade available commercially.

A549 cells (passage 80) from the American Type Culture Collection (ATCC, Rockville, MD, USA) were cultured in Ham's F12-K medium (Sigma), supplemented with 10% fetal bovine serum (Gibco BRL Life Technology, Grand Island, NY, USA), 100 μg/mL each of penicillin G, and streptomycin sulfate (Sigma) at 37°C in 95% air/5% CO_2 environment.

Preparation and Characterization of FITC-Labeled Chitosan Nanoparticles

The synthesis of FITC-labeled chitosan was based on the reaction between the isothiocyanate group of FITC and the primary amino group of chitosan (11). Dehydrated methanol (100 mL), followed by 2.0 mg/mL of FITC in methanol (50 mL), was added into 1% w/v chitosan hydrochloride in 0.1 M acetic acid solution (100 mL). After 3 h of reaction in the dark at ambient temperature, the FITC-labeled chitosan was precipitated in 0.2 M NaOH and separated from unreacted FITC in a Sephadex® G-50 column (2.6 cm I.D. × 40 cm) with 1/15 M phosphate buffer/0.2 M NaCl (pH 5.5) as elution solvent. Fractions containing the labeled polymer were collected with the aid of a FRAC-100 Fraction Collector (Amersham Pharmacia Biotech, Little Chalfont, Buckinghamshire, UK) and a fluorometer (Perkin-Elmer LS-5B, Beaconsfield, Buckinghamshire, UK, λ_{exc} 490 nm, λ_{emi} 520 nm), and dialyzed in 4 Liters of distilled water for 3 days under darkness before freeze drying (Dynavac Engineering, Auckland, New Zealand).

To determine the labeling efficiency, the fluorescence intensity of a solution of FITC-chitosan dissolved in 0.1 M acetic acid and diluted 500× with phosphate buffer, pH 8, until a final concentration of 0.5 μg/mL was measured. Labeling efficiency (percent) was calculated as the percent weight of FITC to weight of the FITC-chitosan. The fluorometer was calibrated with standard solutions of 0.002 to 0.08 μg/mL of FITC prepared by diluting 100 μg/mL methanolic solutions of FITC with phosphate buffer, pH 8.0.

Chitosan nanoparticles were prepared by ionotropic gelation with negatively charged TPP ions according to a previously reported procedure (14). The nanoparticles were obtained by slowly adding 4 mL of 0.10% TPP in water to 8 mL of 0.25% FITC-chitosan in 0.1 M acetic acid with stirring at 1000 rpm (Corning Stirrer/Hot Plate, Corning, NY, USA) at ambient temperature. The nanoparticles were characterized and used for uptake studies immediately upon preparation.

Size and zeta potential of the nanoparticles were analyzed in triplicates by photon correlation spectroscopy and laser Doppler anemometry, respectively, using a particle sizer (Zetasizer 3000 HAS, Malvern Instruments Ltd, Malvern, Worcestershire, UK). *In vitro* release of FITC was determined by incubating at 37°C 1 mL of nanoparticle suspension (1.67 mg/mL) with an equal volume of phosphate buffer, pH 7.4, or transport medium, pH 6.2. At predetermined time intervals, triplicate samples were centrifuged for 30 min at 70,000*g* (Avanti J-25 centrifuge, Beckman Coulter Inc., Fullerton, CA, USA) and the concentration of FITC in the supernatant measured in the fluorometer (Perkin-Elmer). The fluorometer was calibrated with standard solutions containing 0.002 to 0.08 μg/mL of FITC dissolved in the supernatant generated from 1:1 v/v mixtures of unlabeled chitosan nanoparticle suspension and the appropriate dissolution medium that underwent the same procedures as above. Analyses were performed in triplicates.

Uptake Studies

A549 cells of passages 82–90, plated at a density of 1.6×10^5 cells/cm^2 in Multiwell 12-well plates, were used for uptake studies on days 4 and 5 of culture when they formed confluent monolayers. Dosing solutions consisted of freshly prepared FITC-chitosan nanoparticle suspension or FITC-chitosan solution (8 mL of 0.25% solution of FITC-chitosan in 0.1 M acetic acid mixed with 4 mL of water) diluted with the transport medium to give equivalent chitosan concentrations of 0.2 to 1.0 mg/mL. All dosing solutions were adjusted to pH 6.2 with 1 M NaOH. Each cell monolayer was rinsed thrice and pre-incubated for 1 h with 1 mL of transport medium at 37°C. Uptake was initiated by exchanging the transport medium with 1 mL of specified dosing solution and incubating the cells at 37°C for 0.5 to 4 h. The experiment was terminated by washing the cell monolayer three times with ice-cold phosphate-buffered saline (PBS, prepared by dissolving NaCl [8 g/L], KCl [0.2 g/L], Na_2HPO_4 [1.44 g/L], and KH_2PO_4 [0.24 g/L]in water at pH 7.4) and lysing the cells with 1 mL of 0.5% Triton X-100 in 0.2 N NaOH. Cell-associated chitosan was quantified by analyzing the cell lysate in a fluorescence plate reader (Spectra Fluor, Tecan Group Ltd., Männedorf, Switzerland, λ_{exc} 485 nm, λ_{emi} 535 nm) calibrated with standard solutions containing 3.47 to 55.47 μg/mL of FITC-chitosan nanoparticles or chitosan molecules in a cell lysate solution (2×10^5 untreated A549 cells dissolved in 1 mL of the Triton X-100 solution). Uptake was expressed as the amount (μg) of chitosan associated with unit weight (mg) of cellular protein. The protein content of the cell lysate was measured using the Micro BCA protein assay kit (Pierce Chemical Company, Rockford, IL, USA).

Uptake experiments were also conducted with transport media containing either 0.45 M of sucrose, 6 μg/mL of chlorpromazine, 1 μg/mL of filipin, or 0.5 to 6.0 mg/mL of dissolved chitosan hydrochloride. Cells were pre-incubated with 1 mL of the specified medium for 1 h at 37°C before incubation for 2 h with 1 mL of 0.5 mg/mL FITC-chitosan nanoparticles or FITC-chitosan molecules in the same medium. To determine the effect of potassium depletion, a K^+-free buffer solution (140 mM NaCl, 20 mM HEPES, 1 mM $CaCl_2$ and 1 mg/mL glucose, pH 6.2) served as the transport medium and the cells were preincubated in this medium for 3 h at 37°C before uptake experiments performed in the same medium.

Confocal Microscopy

A549 cells of passage 82 were seeded on Lab-Tek® chambered cover glasses (Nalge Nunc International, Naperville, IL, USA) at a density of 1×10^5 cells/cm^2 and incubated at 37°C in 95% air/5% CO_2 environment overnight. The cells

were rinsed twice with prewarmed transport medium and preincubated for 30 min at 37°C with 0.2 mL of transport medium before they were incubated for 1h at 37°C or at 4°C with 0.2 mg/mL FITC-chitosan nanoparticles or FITC-chitosan molecules in the transport medium (0.2 mL). Uptake was terminated by washing the cells three times with ice-cold PBS. The cells were fixed in 3.7% paraformaldehyde, stored overnight at 4°C in Jung® tissue-freezing medium (Leica Instruments, Nussloch, Germany), and examined under an inverted confocal laser scanning microscope (Zeiss Axiovert 200M, Carl Zeiss, Oberkochen, Germany) equipped with an imaging software (LSM 5 Image Browser, Carl Zeiss).

Statistical Analyses

All experiments were repeated at least three times. Results are expressed as means ± standard deviation. Uptake data were analyzed by one-way ANOVA with post-hoc Tukey's tests applied for comparisons of several (≥3) group means (SPSS 10, SPSS Inc., Chicago, IL, USA). A difference between means was considered significant if the p value was less than or equal to 0.05.

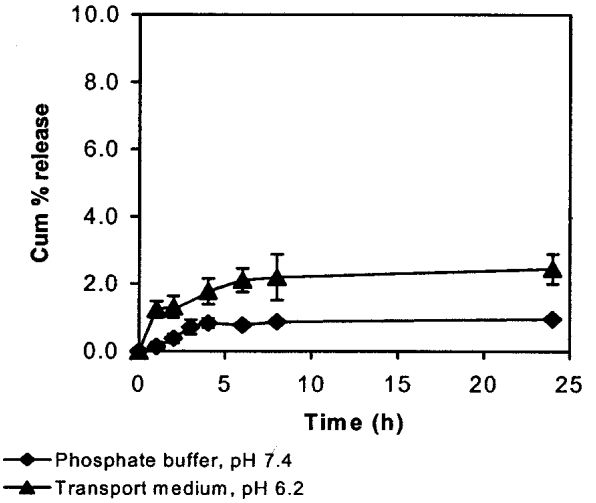

Fig. 1. *In vitro* cumulative percent release of FITC from FITC-labeled chitosan nanoparticles incubated at 37°C with phosphate buffer solution (pH 7.4) and transport medium (pH 6.2). Mean ± SD, n = 3.

RESULTS

The weight fraction of FITC per unit weight of chitosan was 2.7% (w/w). Fluorescence intensity (F) in the cell lysate solution varied linearly with concentration (C) of the FITC-chitosan in the range of 3.47 to 55.47 μg/mL, obeying the relation of $F = 18.44\ C - 41.05$ ($R^2 = 0.995$). The FITC-chitosan conjugate was successfully transformed by ionotropic gelation with TPP into nanoparticles with a mean diameter of 194.7 ± 1.6 nm and zeta potential of +35.5 ± 3.1 mV. Nanoparticles of unlabeled chitosan hydrochloride manufactured under the same conditions had zeta potential of +47.8 ± 0.6 mV, indicating a higher charge repulsion in the chitosan salt, which may account for the nanoparticles having a larger size of 223.2 ± 4.31 nm. Unlike the chitosan hydrochloride salt, the FITC-chitosan was recovered as a base, which might account for the difference in zeta potential between the labeled and unlabeled chitosan nanoparticles. Incubating the labeled chitosan nanoparticles with the phosphate buffer (pH 7.4) or transport medium (pH 6.2) at 37°C resulted in the release of 1 and 2%, respectively, of the conjugated FITC over 24 h (Fig. 1). The FITC conjugation to chitosan in the labeled nanoparticles was stable when diluted with these two aqueous media.

A linear calibration graph ($F = 17.21\ C - 34.81$, $R^2 = 0.995$) was obtained with standard solutions containing 3.47 to 55.47 μg/mL of FITC-chitosan nanoparticles in the cell lysate solution. Prolonged incubation of 6.92, 27.68, and 34.66 μg/mL of FITC-chitosan nanoparticles in the cell lysate solution produced variation in fluorescence intensity, although the coefficients of variation were <10% over 6 h. Thus, solutions in subsequent uptake experiments were analyzed immediately upon cell lysis to avoid this time-dependent variation in fluorescence measurement.

Uptake of the FITC-chitosan nanoparticles by the A549 cells was concentration-dependent, the uptake amount increasing by 2.3-fold when dosing concentration was increased from 0.2 to 1.0 mg/mL (Fig. 2). The same trend was seen of FITC-chitosan molecules, which showed a higher increase in uptake (3.15-fold) over the same concentration range. At 0.2 mg/mL, uptake of the nanoparticles was 1.81-fold higher than that of the chitosan molecules. The uptake ratio of chitosan nanoparticles to chitosan molecules decreased to 1.32 when the dosing concentration was increased to 1.0 mg/mL.

Analysis by fluorometry could not differentiate between intracellular and surface located FITC-chitosan. There was, however, a significant reduction ($p < 0.05$) in chitosan nanoparticle uptake by the A549 cells at 4°C, with the uptake being reduced to 15–18% of that at 37°C at equivalent dosing concentrations (Fig. 2). Uptake of chitosan molecules was similarly temperature-dependent, although it was inhibited by

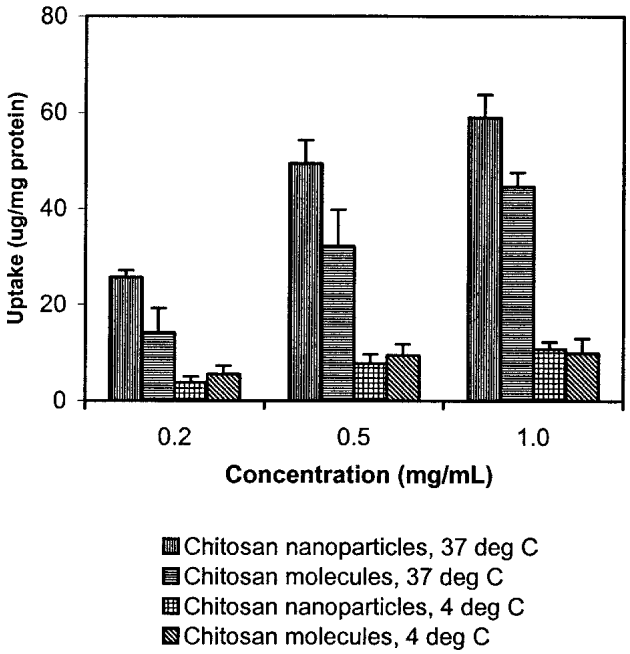

Fig. 2. Two-hour uptake of FITC-chitosan nanoparticles and FITC-chitosan molecules by A549 cells as a function of incubation temperature and dosing concentration. Mean ± SD, n = 4.

a lesser extent at 4°C, exhibiting uptake at 22% (at 1 mg/mL) to 39% (0.2 mg/mL) of those at 37°C (Fig. 2). These results suggest that energy-dependent endocytic processes could be responsible for up to 85% of the chitosan nanoparticles, and up to 78% of the chitosan molecules, associated with the A549 cells at 37°C. Uptake of nanoparticles and chitosan molecules at corresponding concentrations was similar at 4°C ($p > 0.05$), implying that the two forms of chitosan had similar degrees of adhesion to the A549 cells. This physical adsorption increased with dosing concentration to reach a limiting capacity of about 10 μg of chitosan per mg cellular protein (Fig. 2).

Uptake of chitosan nanoparticles by the A549 cells at 37°C increased linearly ($R^2 > 0.95$) with incubation time over 4 h (Fig. 3). The rate of uptake increased by 2.3-fold as concentration was raised from 0.2 mg/mL to 0.75 mg/mL (Fig. 4), and the process seemed saturable at higher concentrations. There was a good fit when the data were transformed to the Michelis-Menten equation ($R^2 = 0.993$), yielding K_m of 692 μg/mL and V_{max} of 58.14 μg/mg/h.

Hyperosmolarity, chlorpromazine (6 μg/mL) and K^+ depletion are known to inhibit clathrin-related processes (15–19). These inhibiting conditions reduced the A549 uptake of the nanoparticles by 65, 34, and 54%, respectively (Fig. 5) but did not totally abolish active internalization of the nanoparticles when compared to uptake at 4°C. Filipin (1 μg/mL), an inhibitor of caveolae-mediated transport processes (20), did not affect nanoparticle uptake by the A549 cells ($p > 0.05$). Neither did it affect the A549 uptake of the chitosan molecules. Of the 3 conditions used to inhibit clathrin-related processes, hyperosmolarity and K^+ depletion significantly reduced the A549 uptake of the chitosan molecules, but chlorpromazine at 6 μg/mL had no significant effect on the uptake (Fig. 5). There was no significant difference between the quantities of cell-associated chitosan nanoparticles and cell-associated chitosan molecules in the presence of hyperosmolarity, chlorpromazine (6 μg/mL) and K^+ depletion (Fig. 5),

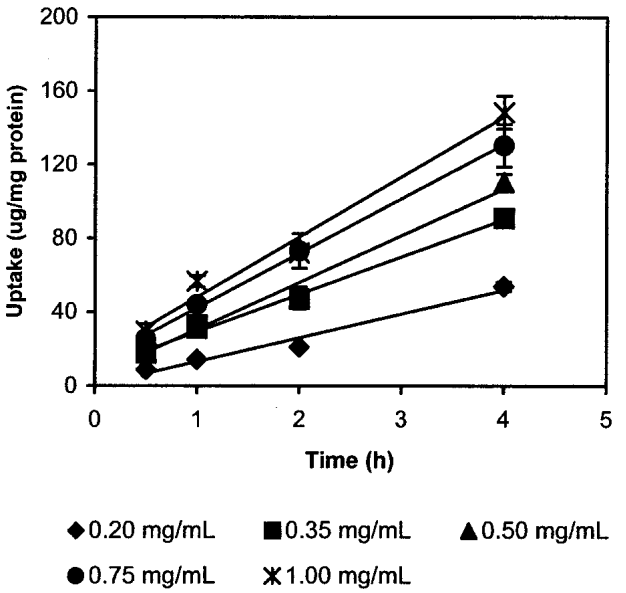

Fig. 3. Time courses for uptake of FITC-chitosan nanoparticles at various dosing concentrations (0.20 to 1.00 mg/mL) by A549 cells at 37°C. Data represents mean ± SD, n = 4.

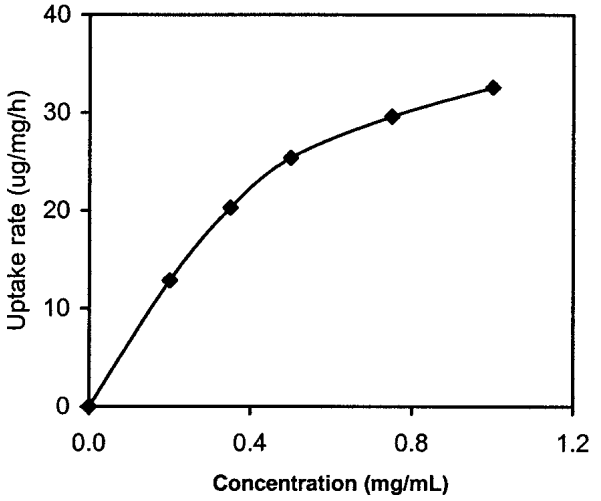

Fig. 4. Rate of uptake of FITC-chitosan nanoparticles by A549 cells after 4 h incubation at 37°C as a function of dosing concentration.

which may suggest a common uptake mechanism for the two forms of chitosan. However, unlabeled chitosan hydrochloride molecules up to a concentration of 6 mg/mL failed to inhibit the uptake of FITC-nanoparticles by the A549 cells (Fig. 6). By contrast, chitosan molecules at 6 mg/mL significantly increased the cellular uptake of the labeled nanoparticles.

Confocal imaging of the A549 cells after uptake experiments supported the quantitative data generated from the uptake studies. The micrographs in Fig. 7 represent the optical sections (x-y axis) of A549 cells after 1 h co-incubation with FITC-chitosan nanoparticles and FITC-chitosan molecules. Cells incubated with the chitosan nanoparticles at

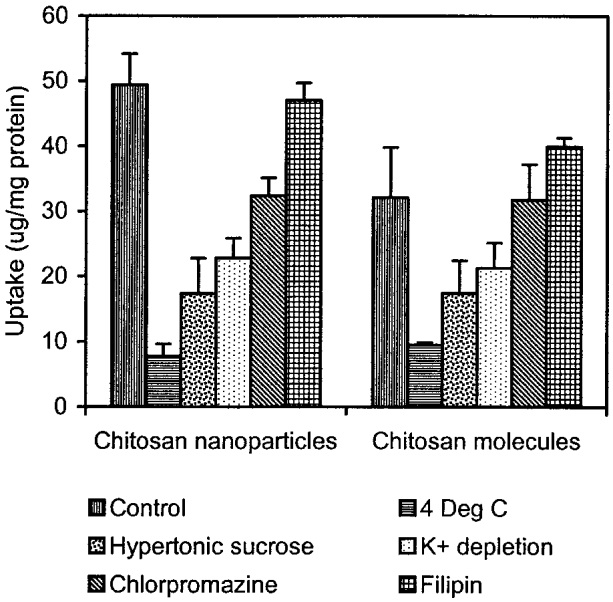

Fig. 5. Uptake of FITC-chitosan nanoparticles and FITC-chitosan molecules by A549 cells at 37°C (control), at 4°C, and at 37°C in the presence of hyperosmolar 0.45 M sucrose medium, 6 μg/mL of chlorpromazine, K^+ free medium, and 1 μg/mL of filipin. Incubation time was 2 h and the dosing concentration was 0.5 mg/mL. Mean ± SD, n = 4.

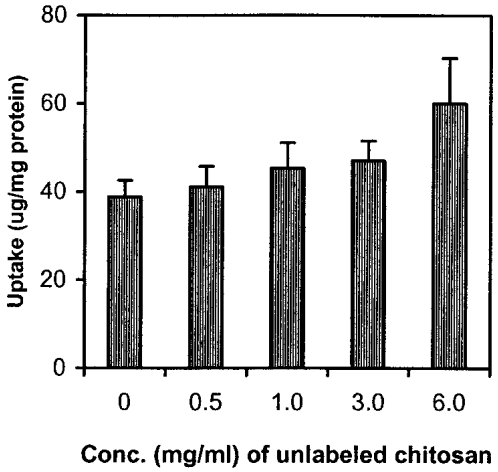

Fig. 6. Uptake of FITC-chitosan nanoparticles by A549 cells in the presence of increasing concentrations of unlabeled chitosan hydrochloride molecules. Uptake was measured after 2 h incubation with 0.5 mg/mL of labeled nanoparticles at 37°C. Mean ± SD, n = 4.

37°C (Fig. 7a) exhibited a thicker layer of stronger fluorescence than cells incubated under the same conditions with the chitosan molecules (Fig. 7b). However, there was no apparent difference in the pattern and intensity of fluorescence shown by these two groups of cells when the uptake temperature was lowered to 4°C (Fig. 7 c and d). In both cases, a thin fluorescent layer coincident with the cell outline was observed. Fluorescence was not detected in control cells that had not been exposed to the FITC-chitosan nanoparticles or FITC-chitosan molecules. A three-dimensional analysis of the confocal data, in particular the reconstruction of the z-axis, indicated that fluorescent signals were located within the cells incubated with the FITC-chitosan nanoparticles at 37°C (Fig. 8). This implicates the internalization of the chitosan nanoparticles by

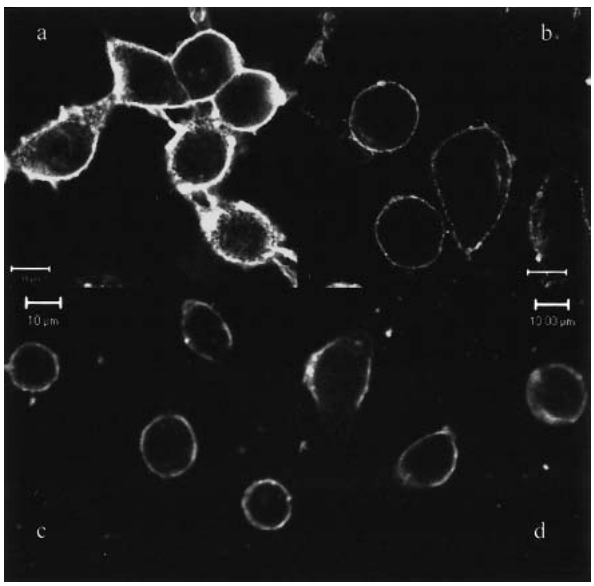

Fig. 7. Confocal images of A549 cells incubated for 1 h with 0.2 mg/mL of FITC-chitosan nanoparticles or FITC-chitosan molecules at different temperatures: (a) chitosan nanoparticles, 37°C; (b) chitosan molecules, 37°C; (c) chitosan nanoparticles, 4°C; (d) chitosan molecules, 4°C.

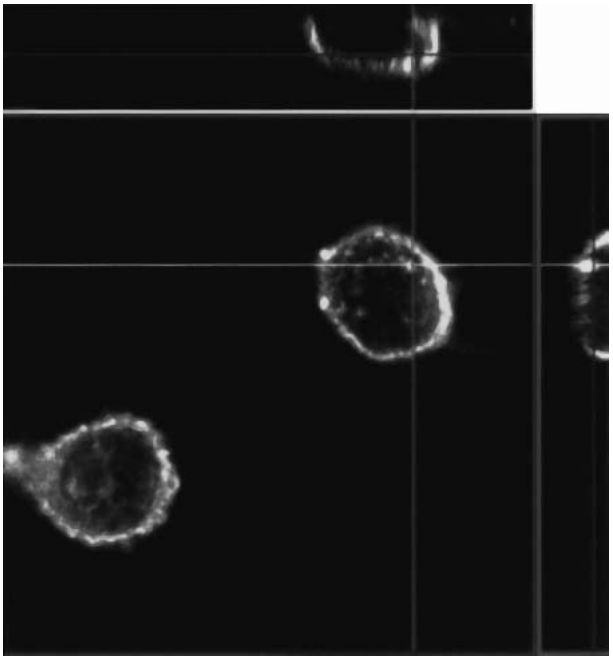

Fig. 8. Optical section (x, y-axis), with respective projections of the x, z- and y, z-axes, of A549 cells incubated for 1 h at 37°C with 0.2 mg/mL of FITC-chitosan nanoparticles. The cross points represent internalized FITC-chitosan nanoparticles.

the A549 cells. Internalization of the chitosan molecules at 37°C could not be confirmed due to the weak fluorescence obtained.

DISCUSSION

Although several pathways for transporting xenobiotics exist in an absorptive epithelium, it is unlikely that significant amounts of chitosan molecules or nanoparticles were transported by passive diffusion via the transcellular and paracellular routes. Even if chitosan were to open up the tight junctions, the uptake of particles >50 nm could not be explained by a widening of the intercellular spaces (7). On the other hand, vesicular endocytic pathways are widely reported to transport macromolecules and particles across absorptive epithelial cells (7,23). In this study, the internalization of the FITC-chitosan nanoparticles by the A549 cells at 37°C was demonstrated by confocal microscopy.

Because the uptake of the FITC-chitosan nanoparticles by the A549 cells was a termperature- and concentration-dependent saturable event, the nanoparticles were unlikely to be internalized by fluid-phase endocytosis, a constitutive process in cells (21). Of the two energy-dependent, saturable endocytic pathways, receptor-mediated endocytosis is initiated by ligand binding to specific cell membrane receptors, whereas adsorptive endocytosis (AE) is preceded by nonspecific interaction of ligand with the cell membrane. Chitosan is known to interact with cell membranes by nonspecific electrostatic forces of attraction (1), and no receptor specific to chitosan has been reported to exist in cell membranes. Moreover, the affinity constant for the uptake of chitosan nanoparticles was 692 μg/mL, equivalent to 3.84 μM, which supports the involvement of AE because substrates transported by receptor-mediated endocytosis generally have higher af-

finities (K_m value in nM range) than those taken up by AE (K_m in μM range; 21).

At 4°C, there was no difference between the degrees of adhesion of chitosan nanoparticles and chitosan molecules to the A549 cells. Both forms of chitosan exhibited concentration-dependent adhesion to the cells, which might be related to a lowering of their zeta potential with dilution because chitosan is reported to interact with epithelial cell membrane by a charge-dependent mechanism (1). The zeta potential of chitosan decreased upon dilution with the transport medium because of a rising ratio of counterions to polymer, which would have contributed to a more effective screening of surface charges on the chitosan. At pH 6.2, the FITC-chitosan nanoparticles showed decreasing zeta potential, from +35.3 ± 3.3 mV to +13.1 ± 0.1 mV, when diluted from 1 to 0.2 mg/mL with the transport medium. The zeta potential of the FITC-chitosan molecules decreased from +28.8 ± 7.5 mV to −4.5 ± 9.5 mV with corresponding dilution. However, chitosan molecules at 0.2 mg/mL, despite having near zero zeta potential, were capable of adhering to the A549 cells with similar tenacities as the positively charged nanoparticles at the same concentration. Uptake of chitosan nanoparticles and chitosan molecules at 4°C was also similar at concentrations of 0.5 and 1 mg/mL, despite their differing zeta potentials. It is therefore possible that other forms of interactions, e.g., H-bonding and hydrophobic interactions, could have contributed significantly to the adhesion of the chitosan nanoparticles and chitosan molecules to the A549 cells.

Several proteins have been identified to regulate cellular trafficking of cargo by endocytosis. The most widely studied is clathrin, which forms coated membrane invaginations on plasma membrane that recruit cell-surface receptors. Plasmalemmal vesicles that use caveolae, macropinosomes or other clathrin-independent pathways can also form at the cell surface to transport molecular cargo (22). Of these, the caveolae are better understood after the identification of the associated protein, caveolin, in the early 1990s. Both the clathrin- and caveolae-mediated endocytic pathways have been implicated in protein transport in mammalian cells (23).

Clathrin was important for the internalization of the chitosan nanoparticles, its inhibition causing up to 65% reduction in nanoparticle uptake by the A549 cells. Inhibition efficiency ranked in the order of hyperosmolarity > K^+ depletion > chlorpromazine, which might be related to the wide range of effects of hyperosmolarity and K^+ depletion on normal cell functions. Chlorpromazine is reported to inhibit receptor recycling by disrupting the assembly-disassembly of clathrin (24). In any case, all three conditions did not completely abolish the internalization of the nanoparticles, suggesting that clathrin independent pathways were probably also involved. Such pathways did not seem to involve caveolae because the nanoparticle uptake was unaffected by filipin, which disrupted caveolae structures by binding and precipitating cholesterol (20). A low expression of caveolin in the A549 cells (25) might have accounted for this lack of involvement of caveolae in the uptake of the chitosan nanoparticles.

The failure of excess unlabeled chitosan molecules to inhibit the A549 uptake of labeled chitosan nanoparticles suggests the absence of a common uptake pathway for the nanoparticles and the chitosan molecules in the cells. Uptake of chitosan by the A549 cells could therefore be sensitive to the form in which the polymer was presented to the cells. The mechanism by which high concentrations of unlabeled chitosan hydrochloride molecules enhanced the uptake of labeled chitosan nanoparticles is not known. Schipper *et al.* (26), using the MTT method, have shown a 40% reduction in intracellular dehydrogenase activity in Caco-2 cells incubated for 1 h with 0.05 mg/mL of chitosan chloride (85% DD, 190 kD) in HBSS (pH 5.5). However, this reduction in enzyme activity is a measure of the impaired metabolism in damaged or dead cells, and could not be associated with enhanced endocytic activity. Although chitosan chloride with high DD (>65%) and high molecular weight (>98kD) could increase the paracellular permeability of Caco-2 cell monolayers at a concentration of 50 μg/mL (26), it remains to be verified that nanoparticles >50 nm could be readily transported through a widening of the intercellular spaces (7). Chitosan at concentrations as high as 10 mg/mL has not been shown to produce significant histologic changes in absorptive cells (26–28). Therefore, it is not likely that the uptake of FITC-nanoparticles by the A549 cells was enhanced by a disruption of the plasma membrane of the cells.

The involvement of clathrin-mediated processes in the uptake of the chitosan molecules is not conclusive, since chlorpromazine did not inhibit this pathway. Uptake of the molecules also did not involve the caveolae-mediated process. A recent review has supported a constitutive clathrin-independent endocytic pathway involved in the trafficking of plasma membrane lipids and markers for lipid rafts from the plasma membrane to the Golgi apparatus in cells (22). This pathway is, however, sensitive to cholesterol and should be inhibited by filipin. Another known clathrin independent pathway is macropinocytosis, where large (up to 5 μm), irregular endocytic vesicles generated at ruffling membrane domains are involved in the non-selective fluid-phase endocytosis of macromolecules (29). Macropinocytosis is prominent in cells with active membrane or cytoskeletal activity, e.g., macrophages and tumor cells, but is present in transformed cells, e.g., MDCK, only after stimulation with growth factors or phorbol esters. Macropinocytosis has not been documented in the A549 cells, but the uptake of large aggregates of titanium dioxide nanoparticles of 50 nm diameter has been observed to occur via membrane-bound phagosomes of >1 μm in the A549 cells (30). Unlike phagocytosis, macropinocytosis is not guided by molecules on the particle surface (29). Further research on the various endocytic pathways, together with the identification of more specific inhibitors for various pathways, would aid in the elucidation of the mechanism of uptake of the chitosan molecules by the A549 cells.

CONCLUSION

Covalent conjugation with FITC yielded fluorescent chitosan molecules, which could be formulated into labeled nanoparticles and enabled the cellular uptake of chitosan nanoparticles and chitosan molecules to be quantified by fluorometry. Formulation of chitosan into nanoparticles enhanced by up to 1.8-fold its uptake by the A549 cells. Uptake of the nanoparticles was not inhibited by co-incubation with excess chitosan molecules, indicating an absence of a common uptake mechanism. A549 uptake of the chitosan nanoparticles was concentration-, and temperature dependent. It increased linearly with time, but showed saturation kinetics at higher concentrations. K_m and V_{max} were 3.84 μM and 58.14

μg/mg/h. Uptake of the nanoparticles at 4°C was less than 18% that at 37°C. Internalization of the chitosan nanoparticles by the A549 cells seems to occur via clathrin-mediated process, but did not involve caveolae-mediated process.

ACKNOWLEDGMENTS

This study was supported by a grant (R148-000-023-112) from the National University of Singapore. Min Huang is grateful to the National University of Singapore for financial support of her graduate studies.

REFERENCES

1. N. G. M. Schipper, S. Olsson, J. A. Hoogstraate, A. G. deBoer, K. M. Vårum, and P. Artursson. Chitosans as absorption enhancers for poorly absorbable drugs 2: Mechanism of absorption enhancement. *Pharm. Res.* **14**:923–929 (1997).
2. N. G. M. Schipper, K. M. Vårum, P. Stenberg, G. Ocklind, H. Lennernäs, and P. Artursson. Chitosans as absorption enhancers of poorly absorbable drugs. 3: Influence of mucus on absorption enhancement. *Eur. J. Pharm. Sci.* **8**:335–343 (1999).
3. A. F. Kotzé, H. L. Lueβen, A. G. deBoer, J. C. Verhoef, and H. E. Junginger. Chitosan for enhanced intestinal permeability: Prospects for derivatives soluble in neutral and basic environments. *Eur. J. Pharm. Sci.* **7**:145–151 (1998).
4. H.-Q. Mao, K. Roy, V. L. Troung-Le, and K. A. Janes, K. Y. Lin, Y. Wang, J. T. August, and K. W. Leong. Chitosan-DNA nanoparticles as gene carriers: Synthesis, characterization and transfection efficiency. *J. Control. Release* **70**:399–421 (2001).
5. L. Illum, I. Jabbal-Gill, M. Hinchcliffe, A. N. Fisher, and S. S. Davis. Chitosan as a novel nasal delivery system for vaccines. *Adv. Drug Deliv. Rev.* **51**:81–96 (2001).
6. K. A. Janes, M. P. Fresneau, A. Marazuela, A. Fabra, and M. J. Alonso. Chitosan nanoparticles as delivery systems for doxorubicin. *J. Control. Release* **73**:255–267 (2001).
7. T. Jung, W. Kamm, A. Breitenbach, E. Kaiserling, J. X. Xiao, and T. Kissel. Biodegradable nanoparticles for oral delivery of peptides: Is there a role for polymers to affect mucosal uptake? *Eur. J. Pharm. Biopharm.* **50**:147–160 (2000).
8. F. Delie. Evaluation of nano- and microparticle uptake by the gastrointestinal tract. *Adv. Drug Deliv. Rev.* **34**:221–223 (1998).
9. K. Suh, B. Jeong, F. Liu, and S. W. Kim. Cellular uptake study of biodegradable nanoparticles in muscular smooth cells. *Pharm. Res.* **12**:1495–1498 (1998).
10. B. Q. Roula and M. A. Mansoor. Synthesis of a fluorescent chitosan derivative and its application for the study of chitosan-mucin interactions. *Carbohydr. Polym.* **38**:99–107 (1999).
11. O. Hiraku and M. Yoshiharu. Biodegradation and distribution of water-soluble chitosan in mice. *Biomaterials* **20**:175–182 (1999).
12. W. Wang, S. Q. Bo, S. Q. Li, and W. Qin. Determination of the Mark-Houwink equation for chitosans with different degrees of deacetylation. *Int. J. Biol. Macromol.* **13**:281–285 (1991).
13. S. C. Tan, E. Khor, T. K. Tan, and S. M. Wong. The degree of deacetylation of chitosan: Advocating the first derivative UV-spectrophotometry method of determination. *Talanta* **45**:713–719 (1998).
14. P. Calvo, C. Remuñán-López, J. L. Vila-Jato, and M. J. Alonso. Novel hydrophilic chitosan-polyethylene oxide nanoparticles as protein carriers. *J. Appl. Polymer Sci.* **63**:125–132 (1997).
15. W. Lutz and R. Kumar. Hypertonic sucrose treatment enhances second messenger accumulation in vasopressin-sensitive cells. *Am. J. Physiol.* **264**:F228–F233 (1993).
16. G. G. Pietra, L. Johns, W. Byrnes, and S. Villaschi. Inhibition of adsorptive endocytosis and transcytosis in pulmonary microvessels. *Lab. Invest.* **59**:683–690 (1988).
17. R. Miñana, J. M. Duran, M. Tomas, J. Renau-Piqueras, and C. Guerri. Neural cell adhesion molecule is endocytosed via a clathrin-dependent pathway. *Eur. J. Neurosci.* **13**:749–756 (2001).
18. I. H. Madshus, K. Sandvig, S. Olsnes, and B. V. Deurs. Effect of reduced endocytosis induced by hypotonic shock and potassium depletion on the infection of Hep 2 cells by picornaviruses. *J. Cell Physiol.* **131**:14–22 (1987).
19. G. Daukas and S. H. Zigmond. Inhibition of receptor-mediated but not fluid-phase endocytosis in polymorphonuclear leukocytes. *J. Cell Biol.* **101**:1673–1679 (1985).
20. P. A. Orlandi and P. H. Fishman. Filipin-dependent inhibition of cholera toxin: Evidence for toxin internalization and activation through caveolae-like domains. *J. Cell Biol.* **141**:905–915 (1998).
21. C. M. Lehr. The transcytosis approach. In A.G. de Boer (ed.), *Drug Absorption Enhancement-Concepts, Possibilities, Limitations and Trends*, Harwood Academic, Switzerland, 1994, pp. 325–366.
22. B. J. Nichols and J. Lippincott-Schwartz. Endocytosis without clathrin coats. *Trends Cell Biol.* **11**:406–412 (2001).
23. J. E. Schnitzer. Caveolae: From basic trafficking mechanisms to targeting transcytosis for tissue-specific drug and gene delivery in vivo. *Adv. Drug Deliv. Rev* **49**:265–280 (2001).
24. L. H. Wang, K. G. Rothberg, and R. G. Anderson. Mis-assembly of clathrin lattices on endosomes reveals a regulatory switch for coated pit formation. *J. Cell Biol.* **123**:1107–1117 (1993).
25. C. Racine, M. Belanger, H. Hirabayashi, M. Boucher, J. Chakir, and J. Couet. Reduction of caveolin 1 gene expression in lung carcinoma cell lines. *Biochem. Biophys. Res. Commun.* **255**:580–586 (1999).
26. N. G. M. Schipper. K. M Vårum and P. Artursson. Chitosans as absorption enhancers for poorly absorbable drugs. 1: Influence of molecular weight and degree of acetylation on drug transport across human intestinal epithelial (Caco-2) cells. *Pharm. Res.* **13**: 1686–1692 (1996).
27. L. Illum, N. F. Farraj, and S. S. Davis. Chitosan as a novel nasal delivery system for peptide drugs. *Pharm. Res.* **11**:1186–1189 (1994).
28. N. Haffejee, J. Du Plessis, D. G. Muller, C. Schultz, A. F. Kotze, and C. Goosen. Intranasal toxicity of selected absorption enhancers. *Pharmazie* **56**:882–888 (2001).
29. J. A. Swanson and C. Watts. Macropinocytosis. *Trends Cell Biol.* **5**:424–428 (1995).
30. R. C. Stearns, J. D. Paulauskis, and J. J. Godleski. Endocytosis of ultrafine particles by A549 cells. *Am. J. Respir. Cell Mol. Biol.* **24**:108–115 (2001).